

Calculation of electric-field gradient in a dilute alloy of Al-Mg

K. K. Prasad Rao and N. C. Mohapatra

Physics Department, Berhampur University, Berhampur-760007, Orissa, India

(Received 21 January 1980)

The existing calculations of electric-field gradient (EFG) in dilute Al-based alloys with nonmagnetic substitutional impurities are unsatisfactory on two accounts. First, the magnitudes of the calculated EFG are very different from the experimental results. Second, these calculations predict an axially symmetric EFG at the nearest-neighbor host sites from the impurity ion, contrary to experimental observations. The discrepancy between experiments and these calculations is largely due to the neglect of the size-effect EFG in the latter. In the present paper, we have calculated in the case of Al-Mg alloy contributions to EFG from both the valence effect and the size effect. The EFG from the valence effect has been calculated from a free-electron-screening charge distribution assumed for the alloy. The size-effect EFG tensor, linear in local strain around the impurity, has been evaluated in the elastic continuum approximation. The present result not only provides improved values for the magnitudes of EFG but also predicts a nonzero asymmetry parameter at the nearest-neighbor host sites from the impurity ion, in fair agreement with experiment.

I. INTRODUCTION

The calculation of the electric field gradient (EFG) in alloys, unlike that in the case of perfect crystals, poses problems. The difficulties arise mainly due to the lack of a good knowledge of the electron distribution in the alloys. The conventional methods of calculating the energy eigenfunctions of electrons in perfect crystals do not apply to the case of alloys on account of the loss of periodicity of the crystal potential in the latter. Under such circumstances, various approximations are made for the screening charge distribution in alloys. We shall discuss here the case of dilute alloys with cubic host and nonmagnetic substantial impurities. In such alloys with aluminum as host, the existing calculations^{1,2} of EFG have been carried out by following either of the two procedures described below.

In the first procedure,¹ a screening charge distribution based on a free-electron model is assumed for the alloy. The scattering phase shifts, in terms of which the screening charge density³ is expressed, are obtained from a scattering potential in the scheme of Alfred and Van Ostenburg.³ In the second procedure,² the screening charge density in the alloy is constructed from a first-order perturbation calculation for the perturbed wave function in the alloy by using an appropriate pseudopotential for the perturbation.

However, the results of calculations for the EFG from either procedure^{1,2} are unsatisfactory in two respects. First, the magnitudes of the calculated EFG are very different from the experimental values.⁴⁻⁶ Second, both these calculations^{1,2} predict an axially symmetric EFG at the nearest-neighbor (NN) host sites, contrary to experiments.⁴⁻⁶ The discrepancy between experi-

ments and these calculations is largely due to the assumptions made in the latter that the EFG arises solely from the valence effect. The latter effect is so called, because its origin is the valence difference of the host and the impurity ions. The other source of EFG, which has been ignored in these calculations,^{1,2} is the lattice strain, resulting from the different sizes of the host and impurity ions. The contribution from the latter source is referred to as the size-effect EFG in literature.⁷

In the case of Cu-based alloys, it is shown by Sagalyn and Alexander⁷ (SA) that the size-effect EFG is even more important than the valence-effect contribution. The latter authors⁷ have shown that by combining the size-effect EFG with the contribution from the valence effect, not only the magnitudes of the calculated EFG are improved but also a nonzero asymmetry parameter results at the NN sites. For the valence-effect contribution, SA (Ref. 7) have used the phase shifts of Hurd and Gordon,⁸ which were obtained for a square-well potential assumed to represent the scattering potential of the impurity ion.

Inspired by the success of these authors⁷ in explaining the observed EFG data in Cu-based alloys, we have made an attempt here to extend their method of calculation to the case of Al-based alloys. Although the present calculation closely resembles those of SA,⁷ there are differences in details; the latter appear particularly in the evaluation of certain parts of the valence-effect EFG.

The motivation for the present calculation is to check whether the procedure of SA,⁷ applied to Al-based alloys, leads to the same success as achieved in the case of Cu-based alloys. As a first step in this direction, we have performed the calculation for the Al-Mg alloy. The results

of this calculation show that the net EFG arising from both the valence effect and the size effect agrees with experiments much better than those from other calculations.^{1,2}

This procedure for calculation,⁷ in principle, can be extended to other alloys of Al with impurities different from Mg. However, results from preliminary calculations for these impurities show that there are some difficulties which limit the accuracy of the calculated EFG. The difficulties arise in the process of solving for a suitable set of phase shifts for these impurities. It is to be remarked here that the standard method of calculating the phase shifts, in the scheme of either Alfred and Van Ostenburg³ or Hurd and Gordon,⁸ is by satisfying both the Friedel sum rule⁷ and the experimental resistivity data⁷ for the alloy. Unfortunately, however, the set of phase shifts so obtained is not unique. This difficulty of nonuniqueness of the set of phase shifts is partially overcome by working with the one set of phase shifts out of all the possible ones which satisfies other experimental data for the alloy in addition to the Friedel sum rule and resistivity data. Such was the case for the phase shifts of Hurd and Gordon⁸ for Cu-based alloys. The experimental data which the phase shifts of Hurd and Gordon⁸ were to satisfy are the fractional solvent Knight shift, the characteristic thermopower, and the change in elec-

tronic specific heat in the alloys.

In the case of Al-based alloys, apart from the resistivity data, the only other experimental data available to our knowledge are the fractional solvent Knight shifts.⁹ Therefore attempts are made in the present calculations to obtain a set of phase shifts which also satisfies the fractional solvent Knight-shift data.⁹ The results of the present calculation show that while this is possible for Mg impurity, it is not so for other impurities in Al-based alloys. Therefore, we have preferred to report the results of the present calculation for Al-Mg only.

The outline of the paper is as follows. Section II contains the derivations of the relevant equations giving the contributions to EFG both from valence and size effects. Results and their discussions are given in Sec. III. The conclusions are summarized in Sec. IV.

II. CALCULATION OF EFG

The calculation of EFG in Al-based alloys closely resembles those of SA (Ref. 7) for Cu-based alloys with some differences in details. The net EFG consists of contributions from both valence effect and the size effect. First, we discuss the contributions from the valence effect.

A. Valence-effect contribution

A free-electron-screening charge distribution is assumed for the alloy. The latter in the large- r region is approximately given^{3,7} by

$$\Delta n(\vec{r}) = - \left(A \frac{\cos(2k_F r + \phi)}{r^3} + B \frac{\cos(2k_F r + \zeta)}{r^4} \right), \quad (1)$$

where the parameters A , B , ϕ , and ζ are known³ functions of the scattering phase shifts and their derivatives with respect to the Fermi wave vector. These phase shifts are calculated from a scattering potential assumed to be either a square well or a square barrier. The latter choice of the potential is determined by the effective valence of the impurity ion in the alloy. The phase shifts are calculated either from the formula¹⁰

$$\tan \eta_l = \frac{j_{l-1}(k_t r_0) j_{l+1}(k_F r_0) - j_{l+1}(k_t r_0) j_{l-1}(k_F r_0)}{j_{l+1}(k_t r_0) m_{l-1}(k_F r_0) - j_{l-1}(k_t r_0) m_{l+1}(k_F r_0)}, \quad (2)$$

in case of both square well and square barrier if $k_t^2 > 0$, or from

$$\tan \eta_l = \frac{k_F I_{l+1/2}(|k_t| r_0) j_{l-1}(k_F r_0) - |k_t| j_l(k_F r_0) I_{l-1/2}(|k_t| r_0)}{|k_t| n_l(k_F r_0) I_{l-1/2}(|k_t| r_0) - k_F I_{l+1/2}(|k_t| r_0) m_{l-1}(k_F r_0)} \quad (3)$$

for a square barrier if $k_t^2 < 0$. Here r_0 is the range of the potential well (barrier). The depth (height) D of the potential well (barrier) is related to k_t by the equation¹⁰

$$k_t^2 = k_F^2 \pm 2D. \quad (4)$$

The plus sign refers to the well and the minus sign

to the barrier. Use of the atomic units ($m = 1$, $\hbar = 1$, $e = 1$) has been made throughout the present calculation. The parameter k_F , used in Eqs. (2)–(4), is the Fermi wave vector for the host metal. The parameters r_0 and D are adjusted to satisfy both the Friedel sum rule including the Blatt correction,¹¹ namely,

$$\Delta Z^* = \frac{2}{\pi} \sum_{l=0}^{\infty} (2l+1)\eta_l, \quad (5)$$

and the experimental resistivity relation

$$\Delta\rho = 0.21749 \left(\frac{4\pi}{Z_h k_F} \right) \sum_{l=1}^{\infty} l \sin^2(\eta_{l-1} - \eta_l), \quad (6)$$

where Z_h denotes the valence of the host ion and η_l is the phase shift in the l th partial wave. The quantity ΔZ^* consists of the sum of two terms, namely, the nominal valence difference between the impurity ion and the host and the Blatt correction¹¹ arising from the change in volume of the impurity cell. It is given in standard notation⁷ by

$$\Delta Z^* = (Z_i - Z_h) - \frac{3}{\gamma_e} Z_h \left(\frac{1}{a} \frac{da}{dc} \right), \quad (7)$$

where Z_i denotes the valence of the impurity ion, and other parameters have their standard meaning.⁷ As remarked before in Sec. I, the set of phase shifts obtained from Eqs. (2)–(7) is, however, not unique. Out of all the possible sets, the one which also satisfies the fractional solvent Knight-shift⁹ data for Al-Mg is chosen for the calculation of EFG.

For the purpose of evaluating the contribution to EFG at the host site in the valence effect, the space around the impurity ion is divided into four regions in exactly the same way as was done by SA (Ref. 7) for Cu-based alloys. The geometry is indicated in Fig. 1. It is easy to see that the EFG at the host site from the charges in region IV is zero.

The EFG from charges in region I is the same as that of a point charge located at the impurity center and with a magnitude equal to the total charge inside the impurity sphere. The latter contribution is given⁷ by

$$q_I^R = \frac{8\pi(1-\gamma_\infty)}{R^3} \int_{R-d/2}^{\infty} r^2 \Delta n(r) dr. \quad (8)$$

The superscript R denotes the axial direction of the valence-effect EFG, and γ_∞ denotes the anti-shielding factor¹² for the host ion.

The contribution to EFG from the charges in region III can be calculated from the standard expression

$$q_{III}^R = \alpha \int_{\text{host sphere}} \Delta n(r) \left(\frac{3 \cos^2 \theta' - 1}{r^3} \right) d^3 r, \quad (9)$$

where α is the so-called Bloch enhancement factor.⁷ In Eq. (9), while r is measured from the impurity ion, r' and θ' are measured from the host ion (see Fig. 1). Equation (9) thus represents a typical two-center integral and can be evaluated by using the technique of α -function expansion of Löwdin.¹³⁻¹⁵ Here we differ with SA (Ref. 7) in the

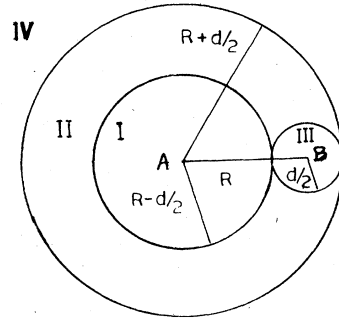


FIG. 1. Geometry used in the calculation of EFG in valence effect. Here A and B denote, respectively, the impurity and host centers.

evaluation of q_{III}^R . The latter authors have used directly the formula for this contribution obtained earlier by Jensen, Nevald, and Williams⁵ (JNW). What JNW did was to calculate the component q_{III}^R (in the direction of the impurity) of the traceless field gradient tensor from the formula⁵

$$q_{III}^R = \alpha \left(\frac{\partial^2 V(r)}{\partial r^2} - \frac{1}{3} \nabla^2 V(r) \right), \quad (10)$$

where $V(r)$ denotes the self-consistent screening potential corresponding to the screening charge $\Delta n(r)$. The expression which they⁵ have used for $V(r)$ is given⁵ by

$$V(r) = \frac{\pi}{k_F^2} \left(\Delta n(r) + \frac{2A \sin(2k_F r + \phi)}{(k_F r^4)} \right). \quad (11)$$

However, the actual self-consistent potential corresponding to the screening charge $\Delta n(r)$ contains more terms involving higher powers of $1/r$ than Eq. (11) gives. Thus, the contribution q_{III}^R obtained from Eqs. (10) and (11) will be limited in accuracy. On the other hand, if one calculates q_{III}^R from Eq. (9), where the charge density instead of potential is used, such errors as associated with the potential of Eq. (11) will not appear. Besides this, Eq. (9) is quite general in the sense that from this the field gradient due to a charge distribution of any kind (not necessarily spherically symmetric as in the present case) can be calculated with the help of α -function¹³⁻¹⁵ expansion.

Expanding $\Delta n(r)$ in terms of α functions¹³⁻¹⁵ centered about the host site and using the orthogonality relations in spherical harmonics, Eq. (9) can be reexpressed as

$$q_{III}^R = \alpha \frac{8\pi}{\sqrt{5}} \int_0^{d/2} \alpha_2 \frac{(N00|R, r')}{r'^2} dr'. \quad (12)$$

Here α_2 is the standard α function¹⁵ corresponding to $l=2$.

The contribution to EFG from charges in region II can be expressed as the difference between two

terms, namely, the contribution from the angular region bounded between the impurity sphere and the outer sphere of radius $R+d/2$ (see Fig. 1) and the contribution from region III. This is expressed as

$$q_{II}^R = (1 - \gamma_\infty) [q_{ann}^R - (1/\alpha)q_{III}^R], \quad (13)$$

where q_{ann}^R denotes the contribution from charges in annular region. The latter can be evaluated from an integral of the same form as given in Eq. (9) but with the range of integration limited to the annular region. Since this integral is a two-center one, it can be converted into a one-center integral by using a suitable transformation. However, unlike expanding $\Delta n(r)$ in the case of q_{III}^R , here the field gradient operator, namely, $(3 \cos^2 \theta' - 1)/r'^3$, which is centered about the host site, is expanded about the impurity site. The standard expansion formula¹⁶ which accomplishes this is given by

$$\frac{P_2(\cos \theta')}{r'^3} = \frac{1}{R^2} \sum_{l=0}^{\infty} \frac{(l+1)(l+2)}{2} \frac{r^l}{R^{l+1}} P_2(\cos \theta) - \frac{4}{3} \pi \delta(\vec{r} - \vec{R}), \quad (14)$$

if $r \leq R$ and by

$$\frac{P_2(\cos \theta')}{r'^3} = \frac{1}{R^2} \sum_{l=2}^{\infty} \frac{l(l-1)}{2} \frac{R^l}{r^{l+1}} P_l(\cos \theta), \quad (15)$$

if $r > R$. Here the function P_l denotes the Legendre polynomial of order l and the δ function is the ordinary Dirac δ function. Substituting Eqs. (14) and (15) in Eq. (9) and integrating over the entire annular region with the help of the orthogonality relations in the Legendre polynomials, the contribution q_{II}^R can be rewritten as

$$q_{II}^R = -8\pi(1 - \gamma_\infty) \times \left(\frac{1}{R^3} \int_{R-d/2}^R r^2 g(r) dr - \frac{1}{3} g(R) + \frac{1}{8\pi\alpha} q_{III}^R \right), \quad (16)$$

where the function $g(r)$ is related to $\Delta n(r)$ and is given by

$$g(r) = A \frac{\cos(2k_F r + \phi)}{r^3} + B \frac{\cos(2k_F r + \zeta)}{r^4}. \quad (17)$$

We would like to remark here that the procedure for evaluating q_{II}^R in the present calculation differs from that of SA.⁷ In order to see the difference between the two procedures, comparison of the results for q_{II}^R and q_{III}^R obtained in both the present procedure and that of SA (Ref. 7) has been made in one sample case of Cu-based alloys. A detailed discussion of this comparison is given in Sec. III.

The net EFG from valence effect is obtained by combining the contributions from all the four re-

gions. The principal components are expressed⁷ as

$$q_{ZZ}^V = q_I^R + q_{II}^R + q_{III}^R + q_{IV}^R \quad (18)$$

and

$$q_{XX}^V = q_{YY}^V = -\frac{1}{2} q_{ZZ}^V. \quad (19)$$

The superscript V stands for the valence effect and the subscripts XX , YY , and ZZ for the principal axes of the valence-effect EFG tensor.

B. Size-effect contribution

The contribution to EFG from size effect has been calculated following the same procedure as that of SA.⁷ Since both Cu and Al hosts have the same cubic structures, the equations derived for the components of the size-effect EFG tensor in the case of Cu-based alloys will hold equally well for Al-based alloys. The principal components of the size-effect EFG tensor at the NN sites are given⁷ by

$$\begin{aligned} q_{xx}^S &= \frac{54\sqrt{2}}{16\pi\gamma_e} \left(\frac{1}{a} \frac{da}{dc} \right) \frac{\Lambda}{d_1^3}, \\ q_{\perp}^S &= -\frac{81\sqrt{2}}{16\pi\gamma_e} \left(\frac{1}{a} \frac{da}{dc} \right) \frac{\Lambda}{d_1^3}, \\ q_{\parallel}^S &= \frac{27\sqrt{2}}{16\pi\gamma_e} \left(\frac{1}{a} \frac{da}{dc} \right) \frac{\Lambda}{d_1^3}. \end{aligned} \quad (20)$$

Similarly the principal components at the next-nearest-neighbor (NNN) sites are⁷

$$q_{\parallel}^S = q_{ZZ}^S = -\frac{108\sqrt{2}}{16\pi\gamma_e} \left(\frac{1}{a} \frac{da}{dc} \right) \frac{\Lambda}{d_2^3} \quad (21)$$

and

$$q_{xx}^S = q_{yy}^S = -\frac{1}{2} q_{zz}^S.$$

Here the lower case letters x , y , and z are used for the crystal coordinates,⁷ whereas the capital letters X , Y , and Z are used to label principal axes of the EFG tensor. The distances d_1 and d_2 are measured from the impurity ion to the respective NN and NNN host ions in the alloy. The subscripts xx , \perp , and \parallel are the principal directions of the size-effect EFG tensor at the NN sites. These are parallel to the respective crystal directions $[100]$, $[0\bar{1}1]$, and $[011]$. Λ is a dimensionless parameter which relates the experimental EFG to the EFG which would be observed if the distorted lattice were made up of unshielded point charges.

Combining the corresponding components of the EFG tensor in the valence effect with those in the size effect, the principal values of the total EFG at the NN sites can be written⁷ as

$$\begin{aligned}
 q_{xx} &= q_{xx}^V + q_{xx}^S = -\frac{1}{2}q_{\parallel}^V + 2q_{\parallel}^S, \\
 q_{\perp} &= q_{\perp}^V + q_{\perp}^S = -\frac{1}{2}q_{\parallel}^V - 3q_{\parallel}^S, \\
 q_{\parallel} &= q_{\parallel}^V + q_{\parallel}^S.
 \end{aligned}
 \quad (22)$$

Similarly the components of the total EFG at the NNN sites are given⁷ by

$$\begin{aligned}
 q_{zz} &= q_{\parallel}^V + q_{\parallel}^S, \\
 q_{xx} &= q_{yy} = -\frac{1}{2}q_{zz},
 \end{aligned}
 \quad (23)$$

where $q_{\parallel}^V = q_{zz}^V$ and is given in Eq. (18). It is clear both from Eq. (23) and also from the symmetry consideration that the total EFG at the NNN sites is axially symmetric with the asymmetry parameter η equal to zero. Equation (22) on the other hand suggests that the total EFG at NN sites is not axially symmetric. Once the parameter Λ is fixed, the principal Z axis as well as the Y and X axes of the total EFG tensor at NN sites can be determined from the standard condition

$$|q_{zz}| \geq |q_{yy}| \geq |q_{xx}|. \quad (24)$$

The asymmetry parameter is then calculated from the relation

$$\eta = (q_{xx} - q_{yy})/q_{zz}. \quad (25)$$

The criterion for fixing Λ is discussed in Sec. III.

III. RESULTS AND DISCUSSIONS

We begin our discussions with the results of EFG from the valence effect. A number of sets of phase shifts satisfying Eqs. (5) and (6) were calculated from either Eq. (2) or (3) depending on whether $k_t^2 > 0$ or $k_t^2 < 0$. Of all these sets, only one had satisfied the fractional solvent Knight-shift data⁹ in Al-Mg. It turned out that for the latter set of phase shifts $k_t^2 < 0$. These phase shifts are therefore calculated from Eq. (3). The derivatives of these phase shifts with respect to the Fermi wave vector, namely $\partial\eta_l/\partial k_F$, are calculated following the same prescription as of Hurd and Gordon.⁸ The set of phase shifts as well as their derivatives up to $l=6$ are summarized in Table I. This table also lists the range r_0 and the height D of the square barrier. The fractional solvent Knight shift, calculated by using these phase shifts, turned out to be 0.012, which is in close agreement with the experimental⁹ value of 0.01.

Using these phase shifts, the contributions q_I^R , q_{II}^R , and q_{III}^R were calculated, respectively, from Eqs. (8), (16), and (12). These results are given in Table II both for NN and NNN sites. For the contribution q_{III}^R , the value of α , the Bloch enhancement factor, used in the present calculation is 7.37. The latter value was obtained from the

TABLE I. Details of phase shifts and their derivatives with respect to the solvent Fermi wave vector. $r_0 = 1.8748$ a.u. and $D = 0.5860$ a.u. Phase shifts are expressed in radians.

l	η_l	$\frac{\partial\eta_l}{\partial k_F}$
0	-0.824 89	-0.668 67
1	-0.319 25	-1.307 84
2	-0.123 99	-0.600 25
3	-0.015 15	-0.106 45
4	-0.000 88	-0.008 22
5	-0.000 03	-0.000 30
6	-0.000 000 7	-0.000 09

works of Holtham and Jena¹⁷ by averaging their \mathbf{k} -dependent enhancement factors over the directions of \mathbf{k} . We would like here to remark that there are available other values, namely $\alpha = 22.6$, 22.8, and 27, of which the first two values have been used in the calculation of Fukai and Watanabe² and the third value by Nevald *et al.*² The values of α used by Fukai *et al.*² were obtained from a single orthogonalized plane-wave (OPW) approximation for the band states. On the other hand, the result of Holtham and Jena¹⁷ for the enhancement factor is based on a many-OPW calculation. In view of this difference in the two methods of calculation, we expect the results of α from the many-OPW calculations¹⁷ to be more accurate than those from a single-OPW calculation.² It is evident from Table II that the magnitudes of q_I^R and q_{II}^R are much smaller than that of q_{III}^R . In fact, the values of q_I^R and q_{II}^R are, respectively, 4.2% and 9.6% of q_{III}^R at NN sites and about 12.4% and 8.4% at NNN sites. Further, the contributions q_{II}^R are opposite in sign to q_I^R at both NN and NNN sites. For the latter reason, the sum $q_I^R + q_{II}^R$ is only 5.4% of q_{III}^R at NN and 3.9% at NNN sites. Somewhat similar results for q_I^R and q_{II}^R were also obtained by SA (Ref. 7) in the case of Cu-based alloys.

It may be recalled here that the present procedures for evaluating the contributions q_{II}^R and q_{III}^R are different from those used by SA (Ref. 7) in Cu-based alloys. It will, however, be interesting to compare the results for q_{II}^R and q_{III}^R obtained in both procedures. For this purpose, we have

TABLE II. Contribution to valence-effect EFG from regions I, II, III, and IV. All the field gradients are given in units of $10^{-3}a_0^{-3}$.

Sites	q_I^R	q_{II}^R	q_{III}^R	q_{IV}^R	$q^R(\text{tot})$
NN	-0.2035	0.4618	-4.8015	0.0	-4.5433
NNN	-0.2447	0.1668	1.9807	0.0	1.9024

picked up the Cu-Zn alloy, as a sample case, for which results of the calculations of SA (Ref. 7) are available. We have also calculated both q_{II}^R and q_{III}^R for the same alloy in the present procedure. In doing so, we have used the same phase shifts and other parameters as used by SA (Ref. 7) in their calculation for Cu-Zn alloy. The results of q_{II}^R and q_{III}^R so obtained for Cu-Zn alloy in both the procedures are summarized in Table III. It is evident from this table that the magnitudes of both q_{II}^R and q_{III}^R in the present calculation are slightly larger than those of SA.⁷ As far as the contribution q_{III}^R is concerned, we have an explanation for this discrepancy.

SA (Ref. 7) have calculated q_{III}^R from the approximate self-consistent potential $V(r)$ of Eq. (11), where terms in $(1/r)$ with powers higher than four are neglected. On the other hand, in the present calculation of q_{III}^R , since $\Delta n(r)$ is used directly in Eq. (9), no such approximation in the self-consistent potential is made. Therefore we expect that the results in the present calculation will be slightly larger in magnitude than those of SA.⁷

In the case of q_{II}^R , we do not have an explanation for the discrepancy between the present results and those of SA,⁷ because the details of calculation of q_{II}^R by the latter authors are not given. Before we begin to discuss the results in the size effect we would like to state that for Al-Mg alloy, we have used in the present calculation $\Delta\rho=0.34$ $\mu\Omega/\text{at.}\%$ for the experimental¹⁸ resistivity and $(1/a)(da/dc)=0.099$ for the fractional change¹⁸ in the lattice parameter per unit concentration of impurity.

The size-effect EFG tensor as given in Eqs. (20) and (21) involves the dimensionless parameter Λ . SA (Ref. 7) have given a prescription to fix Λ in the case of Cu-based alloys. In fact, in their prescription both Λ and α (Bloch enhancement factor) were treated as variable parameters. In the present calculation, we have regarded Λ as the only adjustable parameter. The value of Λ may be fixed in the present case in the following way.

TABLE III. Comparison of the valence-effect contributions q_{II}^R and q_{III}^R for Cu-Zn alloy obtained in the present procedure with those obtained in Ref. 7. All the field gradients are given in units of a_0^{-3} .

Sites	q_{II}^R		q_{III}^R	
	Ref. 7	Present calc.	Ref. 7	Present calc.
NN	-0.01126	-0.01130	-0.00756	-0.00858
NNN	0.00103	0.00107	0.00059	0.00133

The valence-effect EFG calculated from the screening charge $\Delta n(r)$ is expected to give better results at host sites far away from the impurity ion than at NN sites. This is due to the fact that the screening charge density used in the present calculation holds rigorously well only at a far distance from the impurity ion. Thus, one may expect that the valence-effect EFG at the NNN sites will be relatively more accurate than that at NN sites. For this reason, the total EFG at the NNN sites is also expected to be better than that at NN sites. Therefore, the value of Λ may be fixed so as to reproduce the experimental EFG at the NNN sites. Once Λ is fixed this way, it can be used in Eq. (22) to determine q_{ZZ} and η at NN sites. However, still better results of EFG can be obtained if one optimizes the value of Λ so as to minimize the errors in EFG and the asymmetry parameter both at NNN and NN sites. In the case of Al-Mg, the optimum value of Λ is found to be -18.

The components of the size-effect EFG with $\Lambda=-18$, as well as the components of valence-effect EFG, are summarized in Table IV. It is evident from this table that the components of the size-effect EFG are quite large in magnitudes compared to the valence-effect EFG. The relative ratios of the components of the size-effect EFG to valence-effect EFG in the present calculation are similar to those observed in the case of Cu-

TABLE IV. Theoretical values of q and η for Al-Mg alloy. The contributions of the valence and size effects and the principal values of the total EFG tensor are also given. All the field gradients are given in units of $10^{-3}a_0^{-3}$. The largest component is underlined for the purpose of identifying it with the principal z component.

Site	q_{xx}	q_{\perp}	q_{\parallel}	q	η	
NN	Size	-11.2842	16.9272	-5.6430		
	Valence	2.2716	2.2716	-4.5433	19.1988	0.06
	Total	-9.0126	<u>19.1988</u>	-10.1863		
NNN	Size	-4.0779	-4.0779	8.1558		
	Valence	-0.9512	-0.9512	1.9024	10.0582	0.00
	Total	-5.0291	-5.0291	<u>10.0582</u>		

based alloys.⁷ The value of Λ used in the present calculation is well within the range of values of Λ found for Cu-based alloys.⁷

The results of EFG from other calculations^{1,2} as well as those in the present are summarized in Table V. This table also lists the experimental⁴⁻⁶ values of both EFG and the asymmetry parameter in Al-Mg alloy. For reasons already explained in Sec. II, the value of α equal to 7.37 has been used to express the EFG's from other calculations.^{1,2} These are given in columns 2-5 of Table V. It is evident from Table V that the magnitudes of EFG in the present calculation agree with the experimental values⁴⁻⁶ better than those of others.^{1,2} The asymmetry parameter at the NN sites has a value of 0.06 which is well within the range of experimental values.⁴⁻⁶ Further, with the choice $\Lambda = -18$, the agreement of the calculated EFG with the experiment⁴⁻⁶ is very good at the NNN sites. However, at NN sites, there is still a discrepancy of about 35% between the calculated EFG and the experiment.⁴⁻⁶ Of course, here the perfect agreement at NN sites should not be expected, since the screening charge used in the present calculation is not very good at NN sites.

We would like to remark here that results of EFG given in Table V from Refs. 1 and 2 are calculated from the valence effect only. It will be interesting to compare these results^{1,2} with the contributions from the valence effect alone in the present calculation. The latter from Table II are seen to have values -4.5433 and 1.9024 at NN and NNN sites, respectively. Comparing these results with the corresponding results from Refs. 1 and 2 given in Table V, we find that the present results agree better with the results from Ref. 2 both in regard to sign and magnitudes than with the results from Ref. 1. The results from Ref. 1

are opposite in sign to those in the present calculation for both NN and NNN sites. This comparison suggests two things, namely, the phase shifts of Ref. 1 are probably not as good as those in the present calculations. Secondly, the free-electron approximation to the screening charge distribution in Al-Mg is perhaps not so bad an approximation as it was thought by Fukai *et al.*²

The procedure of calculating EFG in Al-Mg can be extended, in principle, to other Al-based alloys with impurities different from Mg. However, as stated before, the phase shifts for these impurities, unlike those of Mg, fail to satisfy the corresponding fractional Knight-shift data.⁹ This failure may be interpreted as an indication of the inadequacy of the free-electron model for the screening charge distribution in Al alloys with these impurities.

IV. CONCLUSION

Following the procedure of Sagalyn and Alexander,⁷ the EFG in dilute Al-Mg alloy has been calculated. The results indicate that the contributions from the size effect are quite important for explaining the discrepancy between the experiments⁴⁻⁶ and the theoretical results from other calculations^{1,2} where this effect has been neglected. In the present calculation, by combining the contributions from valence effect with those from the size effect, not only the magnitudes of EFG's are improved but also a nonzero asymmetry parameter is predicted at NN sites in fair agreement with experiments.⁴⁻⁶

This procedure for calculation⁷ of EFG can be extended, in principle, to dilute alloys of Al with other impurities. However, results from preliminary calculations for these impurities suggest

TABLE V. The total EFG in Al-Mg alloy from theoretical calculations and experiments. The field gradients are given in units of $10^{-3} a_0^{-3}$.

Site	Theoretical ^a					Experiment			
	Ref. 1 ^b q	Ref. 1 ^c q	Ref. 2 ^d q	Ref. 2 ^e q	Present calc. q	η	$ q $	η	Ref.
NN	8.7086	1.0557	-5.6339	-2.3934	19.1988	0.06	27.414	0.12	4
							28.895	0.03	5
							28.895	0.07	6
NNN	-2.8031	-2.4188	1.0061	1.3961	10.0580	0.00	9.335	0.00	4
							9.335	0.00	5
							9.335	0.00	6

^a Asymmetry parameter in the calculations from Refs. 1 and 2 is zero.

^b From the Alfred and Van Osternburg scheme without Blatt correction.

^c From the Alfred and Van Osternburg scheme with Blatt correction.

^d From the calculation of Fukai and Watanabe without exchange correction.

^e From the calculation of Fukai and Watanabe with exchange correction.

that it is difficult to find a suitable set of phase shifts which, in addition to satisfying the Friedel sum rule and the experimental resistivity data, will also satisfy the corresponding fractional solvent Knight-shift data.⁹ In view of this failure, it may be concluded that the free-electron approximation for the screening charge distribution in

the Al-based alloys with these impurities is not good.

ACKNOWLEDGMENT

We are grateful for the support of the University Grants Commission, India, Grant No. 8106.

¹R. Nevald, B. L. Jensen, and P. B. Fynbo, *J. Phys. F* **4**, 1320 (1974).

²Y. Fukai and Kenji Watanabe, *Phys. Rev. B* **2**, 2353 (1970).

³L. C. R. Alfred and D. O. Van Ostenburg, *Phys. Lett.* **26A**, 27 (1967).

⁴M. Minier, *Phys. Rev.* **182**, 437 (1969).

⁵B. L. Jensen, R. Nevald, and D. L. L. Williams, *J. Phys. F* **2**, 169 (1972).

⁶M. Minier and S. Hodung, *J. Phys. F* **7**, 503 (1977).

⁷P. L. Sagalyn and M. N. Alexander, *Phys. Rev. B* **15**, 5581 (1977).

⁸C. M. Hurd and E. M. Gordon, *J. Phys. Chem. Solids* **29**, 2205 (1968).

⁹R. L. Odle and C. P. Flynn, *Philos. Mag.* **13**, 699 (1966).

¹⁰N. F. Mott and H. S. W. Massey, *The Theory of Atomic Collisions* (Clarendon, Oxford, England, 1965).

¹¹F. J. Blatt, *Phys. Rev.* **108**, 285 (1957).

¹²R. M. Sternheimer, *Phys. Rev.* **146**, 140 (1966).

¹³P. O. Lowdin, *Adv. Phys.* **5**, 1 (1956).

¹⁴R. R. Sharma, *J. Math. Phys. (NY)* **9**, 505 (1968).

¹⁵A. Norman Jette, *Int. J. Quantum Chem.* **VII**, 131 (1973).

¹⁶R. M. Pitzer, C. W. Kern, and W. N. Lipscomb, *J. Chem. Phys.* **37**, 267 (1962).

¹⁷P. M. Holtham and P. Jena, *J. Phys. F* **5**, 1649 (1975).

¹⁸Y. Fukai, *Phys. Rev.* **186**, 697 (1969).